

## Discrimination of Diverse (Pressure/Temperature-Dependent/Independent) Inherent Sub-structures in Liquid Water (D<sub>2</sub>O) from Difference Vibrational Spectroscopy

Dimitri E. Khoshitariya,<sup>\*,§,‡</sup> Achim Zahl,<sup>§</sup> Tina D. Dolidze,<sup>‡</sup> Anton Neubrand,<sup>§</sup> and Rudi van Eldik<sup>\*,§</sup>

*Institute for Inorganic Chemistry, University of Erlangen-Nürnberg Egerlandstrasse 1, 91058 Erlangen, Germany, and Institute of Molecular Biology and Biophysics, Georgian Academy of Sciences, Gotua 12, Tbilisi 0160, Georgian Republic*

*Received: June 18, 2004; In Final Form: August 11, 2004*

The new kind of inherent (interstitial) sub-structure of liquid D<sub>2</sub>O under high pressure up to 300 MPa, compared to those found under ambient liquid conditions (5–85 °C) and for D<sub>2</sub>O ice Ih (–10 °C), have been revealed by using of difference and double-difference near-infrared O–D stretching overtone spectroscopy and the subsequent band shape treatment. These procedures rigorously disclosed a variety of component sub-bands exhibiting either dependence on or independence of pressure and temperature. An extended analysis based on the well established correlation between the stretching frequency shift and the hydrogen-bond energy for liquid binary systems (along with the geometric parameters discussed earlier), including also the available results for X-ray and neutron scattering of liquid water, allowed for the identification of basic (Ih ice-like), temperature-induced remote defect (transport-related “tetrahedrally displaced”), temperature-independent dense liquid-phase (probably noncyclic tetramer), and pressure-induced denser (probably cube-like) inherent sub-structures, in accordance with the modern concepts on the liquid–liquid transitions (including the “fragile-to-strong transition” and the “second critical point” hypotheses).

Liquid water and its related physicochemical and biological applications have long been the focus of wide scientific interests. Quite paradoxically, microscopic structural and dynamic properties of liquid water under ambient conditions are much less well-understood as compared to numerous solid forms of water (see refs 1–3 and literature cited therein). The coexistence of at least two different forms of liquid water have been proposed on the basis of indirect experimental,<sup>4</sup> statistical-physical,<sup>5</sup> and molecular dynamics (MD) simulation<sup>6,7</sup> studies but has not been proven conclusively by any experimental method so far. Powerful structural methods, such as X-ray<sup>8,9</sup> and neutron scattering,<sup>10,11</sup> “observe” the appearance of nontetrahedrally arranged “fifth neighbor” (interstitial) or “defect” sub-structures in liquid water as compared to tetrahedrally ordered hexagonal Ih ice crystals,<sup>3</sup> and an increase in the content of these sub-structures on increasing both temperature and pressure.<sup>8–11</sup> Unfortunately, these structural methods do not identify the hydrogen-bonding states of water molecules directly and cannot discriminate whether these interstitial defect molecules are remote or arranged in some kind of cluster. In contrast to structural methods, fundamental and overtone vibrational contours accessible from IR and Raman spectroscopy carry the ultimate information on the nature and distribution of hydrogen-bonded states of all the active oscillators (O–H, O–D) present in the system.<sup>12,13</sup> In this respect, distinct nonlinear correlations between the O–H (O–D) stretching frequency shifts on one hand, and the corresponding hydrogen-bond distances<sup>14,15</sup> and enthalpies<sup>16,17</sup> on another, established for well-characterized solid hydrates and binary liquid-phase systems, respectively, may serve as reliable reference patterns. Indeed, some earlier

spectroscopic studies of liquid water indicated opposite effects of temperature and pressure on hydrogen bonding (strong-to-weak and middle-to-strong transformations, respectively),<sup>18–23</sup> in agreement with general physical considerations.<sup>20</sup> However, either the strategy or the technique for the deconvolution of essentially inhomogeneous (composite) stretching vibrational bands was not sufficient enough in earlier studies<sup>18–23</sup> to obtain quantitatively unequivocal results.

Recently we have introduced an advanced, physically substantiated and rigorous method for the deconvolution of composite vibrational spectral contours based on a combined procedure including the generation of difference and double-difference spectra and a global compositional (Gaussian or similar) analysis.<sup>24,25</sup> In the case of liquid heavy water (D<sub>2</sub>O), we have disclosed five types of O–D oscillators, three of which are of major importance for liquid water under ambient conditions.<sup>24</sup> *In the present letter, we present the new results obtained from high-pressure optical measurements (obtained by exploiting of a new setup<sup>26</sup>) and the comparative analysis of these results in combination with the earlier data<sup>24</sup> that enables the severe discrimination of multiple sub-structures in liquid water and the temperature- and pressure-induced liquid–liquid transitions between them.*

For the first time Figure 1 demonstrates the difference in spectral sub-band composition between the liquid and crystalline states of heavy water (D<sub>2</sub>O). It is seen that spectral components 1 and 2 that are present in D<sub>2</sub>O Ih ice, and obviously represent tetrahedrally arranged (crystalline) water, partially persist also in cold liquid D<sub>2</sub>O water. On transition from the liquid to the solid state, spectral components 3 and 5 disappear totally, whereas component 4 disappears almost this way. Quite obviously, all three of these components, including the major liquid-phase components, 3 and 4, represent water molecules involved in nontetrahedral (defect) sub-structures. Our previous

\* Corresponding author. E-mail: dimitri@anorganik.uni-erlangen.de; dimitri.k@joker.ge.

<sup>§</sup> University of Erlangen-Nürnberg.

<sup>‡</sup> Georgian Academy of Sciences.

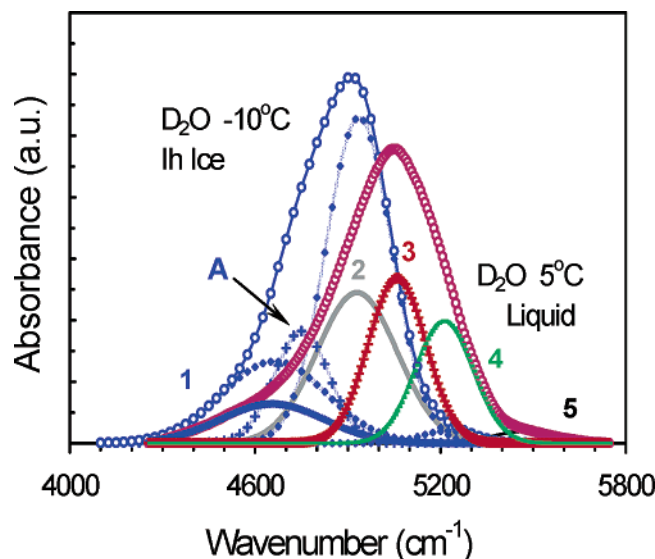


**Figure 1.** Baseline-corrected and normalized experimental (composite) O–D vibrational overtone contours for D<sub>2</sub>O liquid water (open violet circles), and Ih ice (open blue circles; the raw data are taken from refs 24 and 18, respectively). Numbers 1–5 indicate five Gaussian sub-band components corresponding to five different H-bonded states of O–D oscillators in liquid water. These sub-bands are depicted through bold blue and gray curves, red crosses, and green and black (minor band) curves, respectively. The components due to D<sub>2</sub>O ice include those similar to 1, 2, and 4 (blue points), and the component A (blue crosses), not present in liquid D<sub>2</sub>O (not discussed in this paper).

work revealed the following features: (A) The temperature-induced changes in the vibrational contour mostly originates from the redistribution between two major sub-bands, 2 and 4, and to a lesser extent between the sub-bands, 1 and 5.<sup>24</sup> (B) Surprisingly, the contribution of sub-fraction 3 remains constant throughout the entire temperature range.<sup>24</sup> This rather strange behavior of the “central” component of liquid water has been mentioned long ago<sup>18,19,21</sup> but has not been discussed in detail so far (although the “third state” has been outlined<sup>19</sup>). As discussed elsewhere,<sup>24,27–30</sup> the temperature-induced increase in fraction 4 is most probably related to the formation of remote “mobile” defect (interstitial) water molecules, with bifurcated (but not “broken”) hydrogen bonds. These defects can also be defined as “tetrahedral displacements”<sup>29</sup> shaping both dynamic (transport) properties<sup>29–32</sup> and the so-called “fragility” of liquid water<sup>33,34</sup> (see also ref 2).

We will now focus on the origin of sub-band 3 and its relation to the pressure-induced local structural changes in liquid water. Figure 2a demonstrates the results for the effect of 300 MPa pressure on the DO–D stretching overtone vibration spectrum at 25 and 85 °C, respectively. The difference spectra are taken between the pairs of spectra for different pressures (0.1 and 300 MPa) and different temperatures (25 and 85 °C) for the same sample within the high-pressure cell.<sup>26</sup> The difference spectrum due to the temperature-induced changes is reduced by a factor of 3.33 to allow for a direct comparison of intensity redistribution effects. Immediate observations are as follows.

(i) Spectral changes due to an increase in pressure from 0.1 to 300 MPa at 25 °C are very different from those due to an increase in temperature. Here, the pressure increase leads to the appearance of the new band with a maximum at ca. 4800 cm<sup>−1</sup>, which is quite different from the position of the “major” ice-like band at 4935 cm<sup>−1</sup> involved in the temperature-induced rearrangement (Figure 1, Table 1). The “new” band appears at the cost of the decreasing intensity of sub-band 3 that is otherwise essentially insensitive to temperature variation. Actu-

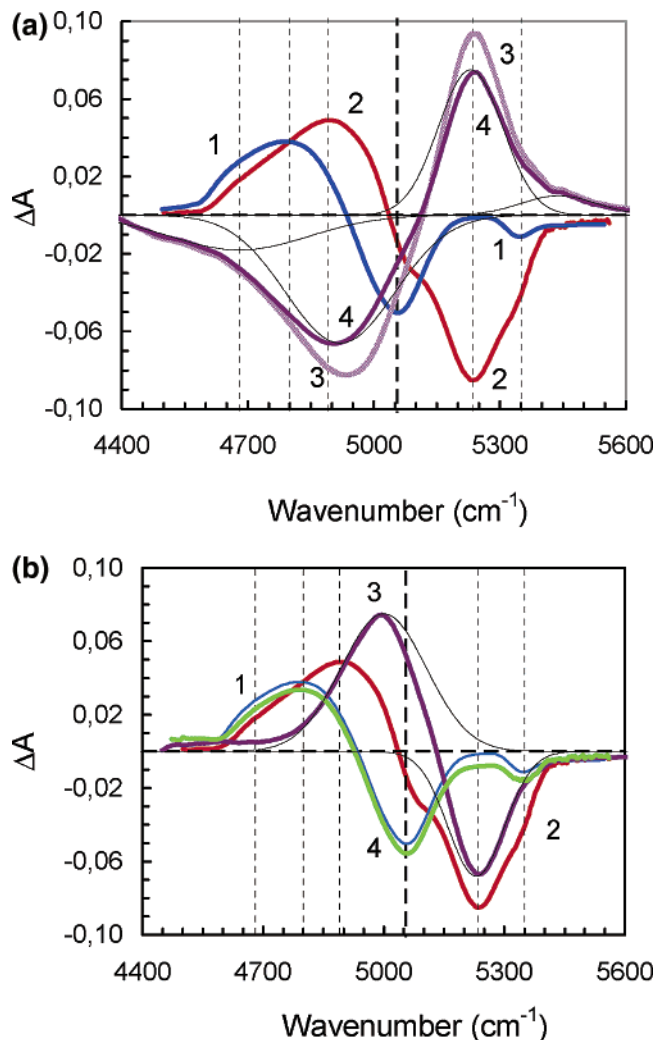


**Figure 2.** (a) Representative difference spectra taken between the pairs of spectra for different pressures and different temperatures. Curves 1 and 2 (depicted in blue and red, respectively): difference spectra between 0.1 and 300 MPa taken at 25 and 85 °C, respectively. Curves 3 and 4 (depicted in light and dark violet, respectively): difference spectra between 85 and 25 °C taken at 0.1 and 300 MPa, respectively. The difference spectrum due to the temperature-induced changes at 0.1 MPa is totally identical to one obtained with a normal cell, ref 24. Thin black curves correspond to the deconvoluted Gaussian component sub-bands 1–5 as depicted in Figure 1 (except the sub-band 3;<sup>24</sup> the difference spectra 3 and 4 were reduced by a factor of 3.33 to allow for the direct comparison of intensity changes). (b) Further treatment of the pressure-related difference spectrum recorded at 85 °C. Curves 1 and 2: same as in (a). Curve 3: difference between curves 4 and 3 of (a). Curve 4: difference between curves 2 and 3 of (a). The overall procedure yields a bright green curve 4, which within the experimental error is identical to the difference curve 1 taken at 25 °C (here and in Figure 2a given in blue). Note, numbering of curves in this figure should not be confused with numbering of sub-bands (components) in Figure 1 and elsewhere in the text.

ally, its maximum position at 5075 cm<sup>−1</sup> is indicative of weakened hydrogen bonding (ca. 4 kcal mol<sup>−1</sup> compared to 5.5 kcal mol<sup>−1</sup> for “normal” hydrogen bonds; see Table 1).

(ii) At higher temperatures, viz., 85 °C, the effect of pressure is somewhat different (Figure 2a); viz., component sub-bands 2 and 4 become pressure dependent. It seems to be similar to, but is probably not just a simple “inversion” of, the temperature effect. Application of double difference analysis revealed the superposition of two effects (Figure 2b), one of which is essentially the same pressure effect as at 25 °C, another constituent indeed being the reverse to the temperature-induced

**TABLE 1: Parameters for the Deconvoluted DO–D and HO–H Stretching Overtone Component Sub-bands under Ambient Conditions A(1)–A(5) (Present Work and Ref 24), for the Pressure-Induced Sub-bands Deduced from Figures 2 and 3 P(1) and P(2) (Present Work, Given in Bold), and the Calculated Matching Parameters for the Fundamental IR and Raman Spectra, the Calculated Hydrogen-Bond Distances, and Calculated Hydrogen-Bond Enthalpies (See Text for Details)**

sub-bands	O–D (O–H) overtone, maximums, cm <sup>−1</sup> (this work, ref 24)	O–D (O–H) overtone, HWMH, cm <sup>−1</sup> (this work, ref 24)	O–D (O–H) fundamental (calcd), cm <sup>−1</sup>	assignment	HB distance, Å (ref 24, this work)	−ΔH <sub>HB</sub> , kcal mol <sup>−1</sup> (this work)
A(1)	4660 ± 10 (6300)	390 ± 20 (530)	2330 (3170)	“strong” tetrahedral (resonance)	2.7 ± 0.05	7.4 ± 0.5
A(2)	4935 ± 10 (6690)	305 ± 10 (415)	2470 (3355) <sup>a</sup>	“normal” tetrahedral	2.8 ± 0.05	5.5 ± 0.5
A(3)	5075 ± 10 (6880)	230 ± 05 (310)	2540 (3450)	“weak” nontetrahedral (planar tetramer)	2.9 ± 0.05	4.2 ± 0.5
A(4)	5230 ± 10 (7085)	200 ± 05 (270)	2610 (3555) <sup>a</sup>	“very weak” displaced (T-bifurcated)	3.0 ± 0.05	2.2 ± 0.5
A(5)	5450 ± 20 (7380)	220 ± 15 (300)	2725 (3707)	“free” (totally broken)	≥ 4.0	≈ 0
<b>P(1)</b>	<b>4800 ± 10</b> <b>(6504)</b>	<b>310 ± 20</b> <b>(420)</b>	2400 (3250)	“strong” nontetrahedral (cubic octamer)	<b>2.75 ± 0.05<sup>b</sup></b>	<b>6.5 ± 0.5</b>
<b>P(2) ≡ A(3)</b>	<b>5075 ± 10</b> <b>(6877)</b>	<b>180 ± 20</b> <b>(245)</b>	2540 (3440)	“weak” nontetrahedral (planar tetramer → cubic octamer)	<b>2.9 ± 0.05<sup>b</sup></b>	<b>4.0 ± 0.5</b>

<sup>a</sup> Experimental data from ref 25. <sup>b</sup> This work.

one. From further comparison of Figure 2a,b and the temperature-related difference spectra published elsewhere,<sup>24,25</sup> it becomes apparent that sub-bands 1 and 5, in contrast to components 2–4 are not pressure dependent even at 85 °C. All in all, it seems that an accumulation of denser inherent heterogeneities (vide infra) with increasing pressure probably leads to the restriction of temperature-induced flip-flop displacements. This competing interplay seems to be responsible for the long discussed anomalous behavior of the transport properties of liquid water during the course of temperature and pressure variation (see, e.g., refs 31 and 32).

Finally, we applied the Badger–Bauer-like analysis to determine the hydrogen-bond enthalpies for the temperature and pressure dependent/independent inherent sub-structures of liquid D<sub>2</sub>O. The most extended and reliable studies revealed the empirical correlation, eq 1,<sup>17</sup> which is essentially nonlinear compared to the Badger–Bauer law proposed earlier.<sup>16,17</sup>

$$-\Delta H_{\text{HB}} = \beta (\Delta\nu - \gamma)^{1/2} \quad (1)$$

Here  $\Delta\nu = \nu_o - \nu_i$  is the frequency shift due to hydrogen bonding (bonded  $\nu_i$  compared to the isolated oscillator,  $\nu_o$ ) and  $\beta$  and  $\gamma$  are the empirical constants.<sup>17</sup>

In Figure 3 the shift of different sub-band positions revealed through the temperature- and pressure-related difference and double-difference procedures (Table 1) were fitted by eq 1 and by simple linear plotting such that the frequency shift for the ice-like component (A2) should correspond to the HB enthalpy of  $-5.50 \text{ kcal mol}^{-1}$ .<sup>27,28</sup> Other values for the HB enthalpies estimated via these two fits are displayed in Table 1. For comparison, Figure 3 displays also the data for a great number of “simple” binar liquid-phase HB systems with O–H groups as HB donors (small asterisks) and the corresponding fit through eq 1 (thin line) with the corresponding values of parameters  $\beta$  and  $\gamma$ .<sup>17</sup> Interestingly, the HB systems with methanol as a HB donor (which is close to the water molecule by electronic structure; indicated by crosses) display considerably better resemblance to our linear and nonlinear fits constructed for different water components.

Results of our analysis based on eq 1 (Figure 3), together with our previous results (Table 1), and the results of relevant X-ray<sup>9</sup> and MD simulation<sup>35</sup> studies, when compared with the available structural and energetic data for small water clusters<sup>36–40</sup> allows for conjecturing structures of inherent dense

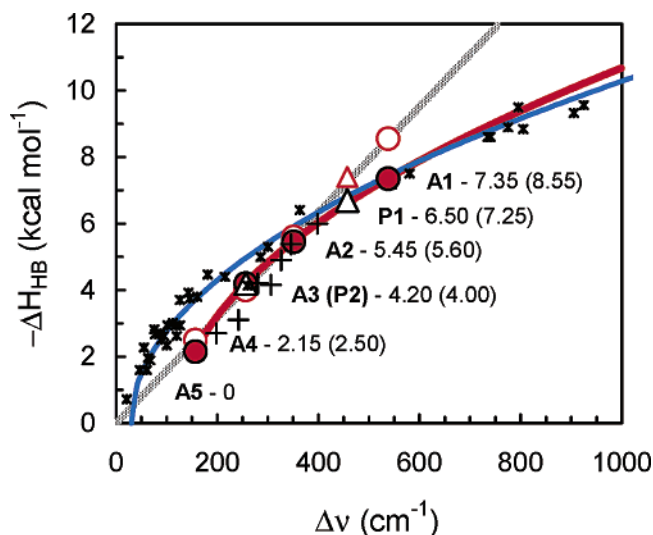


**Figure 3.** Correlations between the O–X (X = H, D) stretching fundamental and overtone band (sub-band) maximum shift (compared to free oscillator) and the HB enthalpy. All band (sub-band) maximum data are normalized to O–H fundamental frequencies via reducing by the factor of 2 (for overtone sub-bands) and/or via escalating by the factor of 1.355 (for O–D fundamental values). Also included are data for the series of well-defined binar liquid systems (crosses, small asterisks and blue curve)<sup>17</sup> and the sub-band maximum shifts for liquid D<sub>2</sub>O (closed red symbols and thick red curve fitted to eq 1) normalized such that for the major ice-like component the HB enthalpy should match the value of  $-5.5 \text{ kcal mol}^{-1}$ . Open symbols and the linear gray plot correspond to the Badger–Bauer-like linear dependence (see Table 1 and Figure 3 for estimated enthalpies). See text for more details.

water components. The tentative assignment is that under ambient conditions, in contrast to the sub-structure related to sub-band 4, sub-band 3 represents another kind of interstitial water molecule apparently arranged in a dense cluster with a hydrogen-bonded structure that differs from the hexagonal arrangement of tetrahedrally connected (low-density) water. Approximately a decade ago, Swishchev and Kusalik<sup>35</sup> on analyzing their MD simulation results, mentioned that some interstitial water molecules should be arranged in four-member rings. Indeed, by considering first of all hexagonal quasi-lattice as a “basic” component of liquid water within a homogeneous mixture model, quasi-planar tetramer clusters can be considered as a second (dense) component that topologically fits best the basic one. This is in agreement with the nontetrahedral



(interstitial) nearest-neighbor separation distance of ca. 3.3 Å.<sup>9,29,35</sup> We found that the individual frequency and the corresponding hydrogen-bond energy values for the “middle” liquid-phase component (3) deduced from our data (Table 1) match those calculated for noncyclic, quasi-planar aqueous tetramer clusters.<sup>36–38</sup> Hence, this structure, having more adaptive nature than the cyclic one, seems to be the most realistic candidate as a dense water sub-structure at ambient pressure. Upon increasing pressure, seemingly another type of even more dense local structure should be formed. The individual frequency of the “appearing” new sub-band and the corresponding hydrogen-bonding energy values nicely resemble the characteristics of a water octamer cubic cluster characterized theoretically<sup>38</sup> and experimentally for the cobalt-containing hydrated solid-phase compound.<sup>39</sup> This cubic octamer, compared to other higher-density water clusters, also fits best the basic ice-like structure. The relatively strong hydrogen bonding in such a dense structure with essentially bent hydrogen-bonded components should be due to the resonance effects within two (of a total of four) cyclic tetramer fragments.<sup>36,37,40</sup> These tetramer fragments are calculated to have resonance (ring) HB distances of  $2.75 \pm 0.05$  Å and HB energies of  $6.5 \pm 0.5$  kcal mol<sup>-1</sup>, matching our values estimated on the basis of difference spectroscopic data (Figure 3, Table 1).

In conclusion, we emphasize that our spectroscopic approach enabled us to disclose and discriminate the fine hydrogen-bonding redistribution effects due to local dense heterogeneities under ambient conditions, and in due course of temperature and pressure variation. Importantly, they also suggest that the two-state approximation is not sufficient for the adequate description of structural, thermodynamic and transport properties of water in the liquid phase.

**Acknowledgment.** This work was supported by the Re-invitation Program of the Alexander von Humboldt Foundation (D.E.K.) and the Deutsche Forschungsgemeinschaft. D.E.K. is grateful to Profs. C. A. Angell, A. Geiger, F. Sciortino, and R. Ludwig for helpful discussions.

## References and Notes

- (1) Debenedetti, P. G. *Metastable Liquids*; Princeton University Press: Princeton, 1997.
- (2) Mishima, O.; Stanley, H. E. *Nature* **1998**, *396*, 329–335.
- (3) Urquidí, J.; Cho, C. H.; Singh, S.; Robinson, G. W. *J. Mol. Struct.* **1999**, *485/486*, 363–371.
- (4) Mishima, O. *J. Chem. Phys.* **1994**, *100*, 5910–5912.
- (5) Ponyatovskii, E. G.; Sinitsyn, V. V.; Pozdnyakova, T. A. *JETP Lett.* **1994**, *60*, 360–364.
- (6) Poole, P. H.; Sciortino, F.; Essmann, U.; Stanley, H. E. *Nature* **1992**, *360*, 324–328.
- (7) Brovchenko, I.; Geiger, A.; Oleinikova, A. *J. Chem. Phys.* **2003**, *118*, 9473–9476.
- (8) Bosio, L.; Chen, S.-H.; Teixeira, J. *Phys. Rev. A* **1983**, *27*, 1468–1475.
- (9) Okhulkov, A. V.; Demianets, Yu. N.; Gorbaty, Yu. E. *J. Chem. Phys.* **1994**, *100*, 1578–1588.
- (10) Bellissent-Funel, M.-C. *Europhys. Lett.* **1998**, *42*, 161–166.
- (11) Soper, A. K.; Ricci, M. A. *Phys. Rev. Lett.* **2000**, *84*, 2881–2884.
- (12) (a) Graener, H.; Seifert, G.; Lauberau, A. *Phys. Rev. Lett.* **1991**, *66*, 2092–2095. (b) Graener, H. *J. Phys. Chem.* **1991**, *95*, 3450–3453.
- (13) Hare, D. E.; Sorensen, C. M. *J. Chem. Phys.* **1992**, *96*, 13–22.
- (14) Novak, A. In *Structure and Bonding*; Dunitz, J. D., Ed.; Springer: Berlin, 1974; Vol. 18, pp 177–216.
- (15) Berglund, B.; Lindgren, J.; Tegenfeldt, J. *J. Mol. Struct.* **1978**, *43*, 179–191.
- (16) Rao, C. N. R.; Dwivedi, P. C.; Ratajczak, H.; Orville-Thomas, W. *J. J. Chem. Soc., Faraday Trans. 2* **1975**, *71*, 955–966.
- (17) Iogansen, A. V. *Spectrochim. Acta A* **1999**, *55*, 1585–1612.
- (18) Luck, W. A. P.; Ditter, W. *Z. Naturforsch.* **1969**, *24B*, 482–494.
- (19) Angell, C. A.; Rodgers, V. *J. Chem. Phys.* **1984**, *80*, 6245–6252.
- (20) Walrafen, G. E.; Abebe, M. *J. Chem. Phys.* **1978**, *68*, 4694–4695.
- (21) Walrafen, G. E.; Yang, W.-H.; Chu, Y. C.; Hokmabadi, M. S. *J. Phys. Chem.* **1996**, *100*, 1381–1391.
- (22) Jin, Y.; Ikawa, S.-I. *J. Chem. Phys.* **2003**, *119*, 12432–12438.
- (23) Kawamoto, T.; Ochiai, S.; Kagi, H. *J. Chem. Phys.* **2004**, *120*, 5867–5870.
- (24) Khoshtariya, D. E.; Dolidze, T. D.; Lindqvist-Reis, P.; Neubrand, A.; van Eldik, R. *J. Mol. Liq.* **2002**, *96/97*, 45–63.
- (25) Khoshtariya, D. E.; Hansen, E.; Leecharoen, R.; Walker, G. C. *J. Mol. Liq.* **2003**, *105*, 13–36.
- (26) Zahl, A.; Igel, P.; Weller, M.; Khoshtariya, D. E.; Hamza, M. S. A.; van Eldik, R. *Rev. Sci. Instrum.* **2003**, *74*, 3758–3762.
- (27) Giguère, P. A. *J. Chem. Phys.* **1987**, *87*, 4835–4839.
- (28) Sciortino, F.; Geiger, A.; Stanley, H. E. *Nature* **1991**, *354*, 218–221.
- (29) Agmon, N. *J. Phys. Chem.* **1996**, *100*, 1072–1080.
- (30) Rønne, C.; Trane, L.; Åstrand, P.-O.; Wallquist, A.; Mikkelsen, K.; Keiding, S. R. *J. Chem. Phys.* **1997**, *107*, 5319–5331.
- (31) Lokotosh, T. V.; Magazu, S.; Maisano, G.; Malomuzh, N. P. *Phys. Rev. E* **2000**, *62*, 3572–3580.
- (32) Geiger, A.; Kleene, M.; Paschek, D.; Rehtanz, A. *J. Mol. Liq.* **2003**, *106*, 131–146.
- (33) Ito, K.; Moynihan, C. T.; Angell, C. A. *Nature* **1999**, *398*, 492–495.
- (34) Angell, C. A.; Bressel, R. D.; Hemmati, M.; Sare, E. J.; Tucker, J. C. *Phys. Chem. Chem. Phys.* **2000**, *2*, 1559–1566.
- (35) Svishchev, I. M.; Kusalik, P. G. *J. Chem. Phys.* **1993**, *99*, 3049–3058.
- (36) Masella, M.; Gresh, N.; Flament, J.-P. *J. Chem. Soc., Faraday Trans.* **1998**, *94*, 2745–2753.
- (37) Xanteas, S. S. *J. Chem. Phys.* **2000**, *258*, 225–231.
- (38) Knochenmuss, R.; Leutwyler, S. *J. Chem. Phys.* **1992**, *96*, 5233–5244.
- (39) Blanton, W. B.; Gordon-Wylie, S. W.; Clark, G. R.; Jordan, K. D.; Wood, J. T.; Geiser, U.; Collins, T. J. *J. Am. Chem. Soc.* **1999**, *121*, 3551–3552.
- (40) Köddermann, T.; Schulte, F.; Huelsekopf, M.; Ludwig, R. *Angew. Chem., Int. Ed.* **2003**, *42*, 4904–4908.